EurJIC
European Journal of Inorganic Chemistry

Full Paper
doi.org/10.1002/ejic.202000068

Chemistry Europe
European Chemical Societies Publishing

Formic Acid Dehydrogenation

Formic Acid Dehydrogenation by a Cyclometalated κ^3-CNN Ruthenium Complex

Alexander Léval,[a] Henrik Junge,[a] and Matthias Beller*[a]

Abstract: Hydrogen utilization as a sustainable energy vector is of growing interest. We report herein a cyclometalated ruthenium complex [Ru(κ^3-CNN)(dppb)Cl], originally described by Baratta, to be active in the selective dehydrogenation (DH) of formic acid (FA) to H_2 and CO_2. TON's of more than 10000 were achieved under best conditions without observation of CO (detection limit 10 ppm). The distinguished behavior of the catalyst was explored varying the starting conditions. Our observation revealed the complex [Ru(κ^3-CNN)(dppb)(OOCH)] as key species in the catalytic cycle.

Introduction

Formic acid (FA) is considered as a benign candidate for the reversible storage of hydrogen which has a promising potential as a sustainable energy source. In this case, FA dehydrogenation and CO_2 hydrogenation are the two antagonist reactions which allow for reversible hydrogen storage[1]. The recent years have seen the development of numerous active catalysts for the homogeneous CO_2 hydrogenation as well as for DH of FA under various conditions. For the latter reaction, intensive work has been carried out on ruthenium[2], iridium[3] and iron[4]. However, the library of active catalysts for this transformation also includes manganese, [5] cobalt[6], copper[7], nickel[8], rhenium[9], rhodium[10], boron[11], aluminum[12] and platinum[13] complexes. Regarding the employed ligands, in the past decade interesting multi-dentate systems were developed which allow for improved catalyst performance. As a result, higher catalyst activities, productivities and stabilities were reached.

Prominent examples utilize so-called non-innocent ligands which enable metal ligand bifunctional catalysis[3]. Generally, these ligands can be classified in categories according to the type and number of chelating sites. For example, in the case of ruthenium-based catalysts, monodentate ligands (κ^1-P), bidentate (κ^2-PP, κ^2-NN), tridentate (κ^3-PNP, κ^3-PNN, κ^3-PP_3), and tetradentate ligands (κ^4-PNNP, κ^4-NP_3) have been applied so far. Notably, those different classes of ligands present unique intrinsic features leading to distinct action modes depending on the applied conditions. Scheme 1 summarizes some preeminent systems described for FA DH spotlighting various ligand classes.

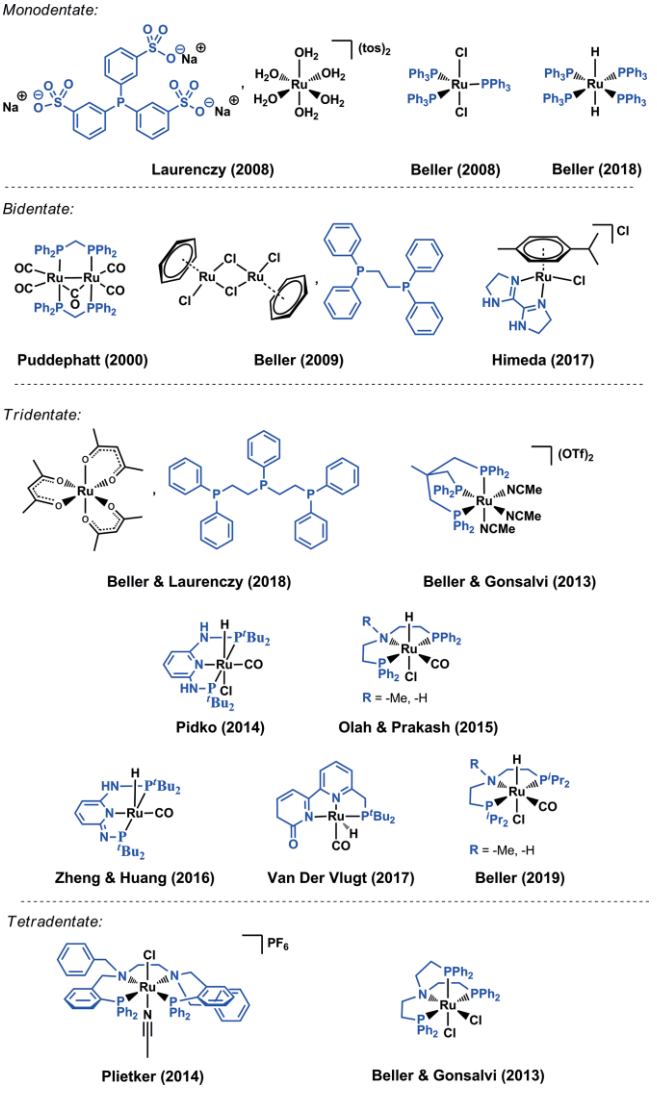

Scheme 1. Selected systems for the Ru catalyzed DH of FA.

[a] *Leibniz-Institut für Katalyse e.V.,*
Albert-Einstein-Straße 29a, Rostock, 18059, Germany
E-mail: matthias.beller@catalysis.de
http://www.catalysis.de

Supporting information and ORCID(s) from the author(s) for this article are available on the WWW under https://doi.org/10.1002/ejic.202000068.

Additionally, a selection of the best catalysts for the FA DH according to the coordination mode of the main ligand (mono-, bi-, tri- and tetradentate) is available in the supporting information (Figure S5).

In 2008, Laurenczy and our group independently reported efficient homogeneous ruthenium catalysts for the FA DH.

In our case [$RuCl_2(PPh_3)_3$] allowed for a TON of 893 in 3 hours[14], while Laurenczy and co-workers developed the water-soluble system consisting of [$Ru(H_2O)_6$](tos)$_2$ with 2 equivalents of 3,3′,3″-phosphane-triyltris(toluenesulfonic acid) trisodium salt (TPPTS) reaching a TON of 460[15]. More recently, the hydride complex [$RuH_2(PPh_3)_4$] was reported as a very active catalyst for FA DH (TON of 1980 in 90 min)[22] Further investigations showed that switching from monodentate to bidentate phosphine ligands even increased the activity. The starting point was settled by Puddephatt with the [$Ru_2(\mu\text{-}CO)(CO)_4(\mu\text{-}dppm)_2$] catalyst (dppm = bis(diphenylphosphino)methane) (TOF of 500 h^{-1})[16]. This was followed by studies on the dimer [{$RuCl_2$(benzene)}$_2$] with 1,2-bis(diphenylphosphino)ethane(dppe) reaching a TON of 1 376 in 180 minutes. In further experiments by our group, the TON and TOF were stepwise improved up to 10^6 and ca. 47000 h^{-1} respectively in continuous flow experiments[16c, 16d, 17]. Himeda and co-workers reported the highly active catalyst [(*p*-cymene)Ru(bisimidazoline)Cl]Cl reaching a TON of 11670 (350000 in continuous flow experiments)[2d]. Based on the recent interest in catalysis using specific pincer complexes[18], also ruthenium-based pincer complexes were reported for the formic acid dehydrogenation such as [(κ^3-PNN)Ru(CO)H] by Van der Vlugt[3]. Interestingly, Olah and Prakash compared the catalytic behavior of [Ru(^{Ph}P^{Me}N^{Ph}P)(CO)ClH] and [Ru(^{Ph}P^{H}N^{Ph}P)(CO)ClH] (TOF of 430 and 298, respectively)[19]. Similar results were obtained by us, using [Ru(^{iPr}P^{Me}N^{iPr}P)(CO)ClH] and [Ru(^{iPr}P^{H}N^{iPr}P)(CO)ClH], which reached TOF's of 9219 h^{-1} and 2573 h^{-1}, respectively empathizing the superiority of methylated PNP ligands for the Ru catalyzed FA DH[25]. Furthermore, κ^3-(^{tBu}P^{H}N^{py}N^{H}N^{tBu}P) ruthenium complexes were described as active for the formic acid dehydrogenation by Zheng and Huang (TOF of 2380 h^{-1})[20] as well as Pidko (TOF = 257000 h^{-1} reached in continuous flow) [21]. Additional phosphine based tridentate ligands were developed such as [$Ru(acac)_3$] in the presence of bis(diphenylphosphinoethyl)phenylphosphine (triphos)[22] or [$Ru(P_3)(MeCN)_3$](OTf)$_2$[23]. Finally, even specific tetradentate ruthenium complexes have been studied for the FA DH. Indeed, Plietker et al. reported the efficient [Ru(κ^4-PNNP)Cl(MeCN)](PF_6) reaching a TON of 5600[2], while Beller and Gonsalvi jointly reported [Ru(κ^4-NP_3)Cl_2] with a TON of 902 h^{-1}[23].

Motivated by designing new catalysts, we became interested by the potential of cyclometalated Ru complexes for FA DH, which was not yet described. The group of Baratta reported the ruthenium complex [Ru(κ^3-CNN)(dppb)Cl] as a very efficient catalyst for transfer hydrogenation (TH) reactions [24]. This work attracted our attention and we anticipated an interesting ligand feature in the Ru catalyzed FA DH with this cyclometalated κ^3-CNN ruthenium complex. Inspired by this and our recent work regarding ruthenium catalyzed decomposition of FA with a [Ru(^{iPr}P^{Me}N^{iPr}P)(CO)ClH] catalyst[25], we investigated the potential of this TH catalyst for FA DH leading to H_2 and CO_2 (Scheme 2).

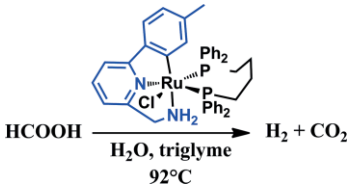

Scheme 2. Purpose of this work.

Results and Discussions

Ligand and Complex Synthesis

The synthesis of the ligand and the complex was made with a slight modification from the procedure as described by Baratta et al [24]. Oxidation of 2-(*p*-tolyl)pyridine **1** with H_2O_2 in acetic acid for 13 hours led to 2-(*p*-tolyl)pyridine-1-oxide **2** with 97 % yield [26]. Cyanation of the oxide compound in the presence of dimethylcarbamic chloride and trimethylsilanecarbonitrile gave cyanopyridine **3** (79% yield) [24]. Finally, hydrogenation of **3** with 10% Pd/C in EtOH afforded the κ^3-CNN ligand **4** in moderate yields (42%) [27]. Reaction between [*trans*-Ru(dppb)(PPh_3)Cl_2] **5** and **4** led to the complex described by Baratta and his group in good yield (91%) (Scheme 3)[29][28].

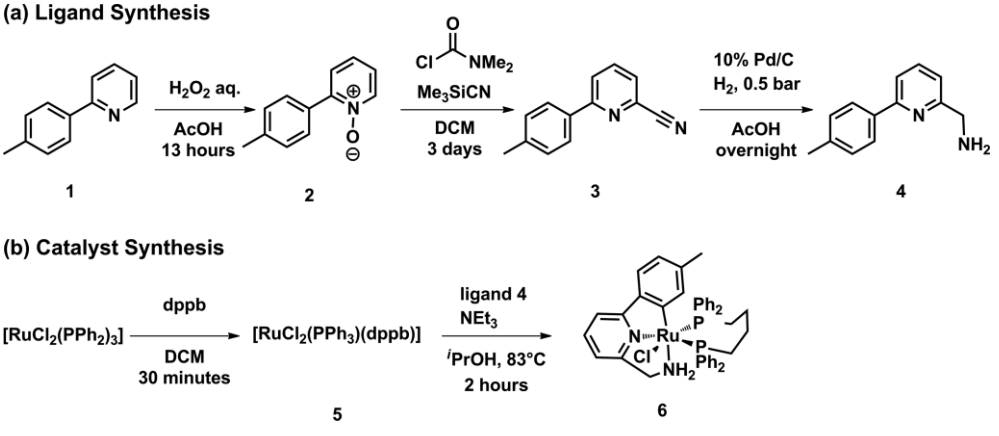

Scheme 3. Synthesis of the ligand and Ru-CNN complex.

Full Paper
doi.org/10.1002/ejic.202000068

Catalytic FA Dehydrogenation

Having complex **6** in hand, we tested FA DH in the conditions previously reported by our group for Ru catalysts [25]. As shown in Table 1, they can be divided in: (i) aqueous based and (ii) amine containing system. The reaction carried out in FA/DMOA (11:10 molar ratio, DMOA = N,N-dimethyloctylamine) afforded 1204 mL of H_2/CO_2 mixture (entry 4). Notably, the catalyst **6** behaves significantly different under aqueous conditions. To have an accurate interpretation of the results, we analyzed the gas evolution plot over the time course of the reaction (Figure S6). Under acidic conditions, **6** (entry 1) enabled a straightforward gas evolution reaching 902 mL (TON of 6155). It is worth mentioning that the solution decolored from yellow to colorless within the first minutes of the reaction. Applying neutral and basic conditions (entries 2 and 3) resulted in increased productivities and activities. Indeed, final TONs of 7414 and 7940, respectively, were reached after 3 hours. As one can expect, the ability of the medium to trap CO_2 (as HCO_3^-) increases from acidic, to neutral, to basic pH. This can be easily observed in the gas chromatography (GC). After 180 minutes, there is significantly less CO_2 in the gas phase if the reaction is carried out in basic pH than in acidic (Table S1). Therefore, even though the gas evolutions are not identical according to the plot (Figure S6), higher catalyst turnover numbers are obtained in neutral and basic media. Here, the color of the solution remained orange throughout the reaction. To demonstrate the stability of this novel FA DH catalyst, a long-term experiment was carried out under neutral conditions (Figure S7). Satisfyingly, almost full conversion was reached in 22 hours resulting in 1338 mL of H_2/CO_2 mixture (ratio vol.%H_2/(vol.%H_2 +vol.%CO_2) = 0.65; yield of 96%, TON of 11910).

To investigate the impact of critical reaction parameters such as temperature, catalyst loading and additive use, further experiments varying the initial conditions were carried out (Table 2). As expected, heating the system enhanced gas evolution over time (Figure S8). Indeed, at 112 °C, a final TON of 10775 was reached in 180 minutes (entry 3). In contrast, a temperature of 72 °C afforded much lower TON (3608) (entry 1). Increasing the catalytic loading was not beneficial. Indeed, 5 μmol of [Ru(CNN)(dppb)(Cl)] yielded a TON of 5666 (entry 5), nearly equivalent to 3 μmol (entry 2, TON of 7414). Interestingly, even 1 μmol of catalyst (entry 4) led to a reasonably satisfying TON (13778) (Figure S9). Additionally, various additives were tested to see if they would enhance the reaction (Figure S10). Lithium tetrafluoroborate slightly improved the catalyst performance with a TON of 8731 (entry 6). However, a high CO content of 253 ppm was noted (Table S1). Addition of lithium chloride resulted in a TON of 8186 over the course of 180 minutes, while no CO was observed (entry 7). Finally, a mixture of HCOONa (32 mmol) and HCOOH (5 mmol) was used instead of HCOOH (37 mmol) and KOH (40 mmol). As expected, almost the same TON (8390) was observed entry 8) [5d].

Mechanistic Investigations: NMR Measurements and X-ray Crystal Structure Analysis

To have more insights under the applied aqueous conditions, NMR experiments with an increased amount of catalyst **6** (40 μmol) under basic (potassium formate) and acidic (formic acid) conditions were carried out.

Table 1. DH of FA using **6**.[a]

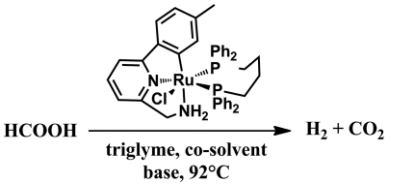

Entry	Base[b]	Co-solvent[c]	Volume [mL][d]	TON[e]	TOF [h^{-1}][f]
1	KOH	H_2O	902	6155	2052
2	KOH	H_2O	817	7414	2471
3	KOH	H_2O	673	7940	2647
4	DMOA	–	1204	8220	2740

[a] Reaction conditions: HCOOH (37 mmol), triglyme (4 mL), base, co-solvent [Ru(CNN)(dppb)Cl] (0.003 mmol), T_{set} (92.5 °C), time (180 min). [b] For entries 1 to 3, base (KOH) amount: 20, 40 and 60 mmol (initial pH of 4.5, 6 and 14, respectively). For entry 4: 11:10 molar ratio of FA/DMOA. [c] For entries 1–3, degassed water (9 mL) was used. [d] Gas evolution monitored with manual burettes, corrected by blank volume (2.2 mL) and content of the gas phase analyzed by gas chromatography (GC). Ratio vol.%H_2/(vol.%H_2 +vol.%CO_2) in all cases 0.5 except entries 2 and 3 (0.67 and 0.87), CO not observed in the gas phase (detection limit 10 ppm) (Table S1). All experiments were performed twice with reproducibility differences between 2.1 and9%. [e] TONs and TOFs calculated based on the measured ratio of H_2/CO_2. [f] TOFs calculated after 3 hours.

Table 2. Temperature, catalyst loading and additive variation for the DH of FA.[a]

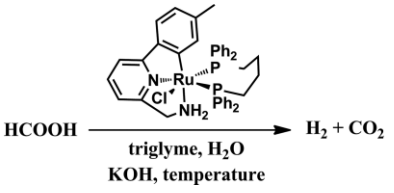

Entry	T [°C]	Cat. loading [μmol]	Additive	TON[c]
1	72	3	KOH	3608
2	92	3	KOH	7414
3	112	3	KOH	10775
4	92	1	KOH	13778
5	92	5	KOH	5666
6	92	3	$LiBF_4$	8731
7	92	3	LiCl	8186
8[b]	92	3	HCOONa	8390

[a] Reaction conditions: HCOOH (37 mmol), triglyme (4 mL), water (9 mL), KOH (40 mmol) or other additives (10 mol-% according to the cat. amount), [Ru(CNN)(dppb)Cl], time (180 min). [b] For entry 8, a mixture of HCOOH (5 mmol) and HCOONa (32 mmol) was used instead of HCOOH (37 mmol) and KOH (40 mmol), to match the starting pH of entry 2. Gas evolution was monitored with manual burettes, corrected by blank volume (2.2 mL) and content of the gas phase analyzed by gas chromatography (GC). Ratio H_2/CO_2 in all cases not 1:1 due to CO_2 being trapped as carbonate (Table S1). CO not observed in the gas phase (detection limit 10 ppm) except from entries 3, 4 and 6 (17, 13, and 253 ppm) (Table S1). Experiments in entries 1–5 were performed twice with reproducibility differences between 0.1 and 3.5% except entry 4 (17.5%). [c] TONs and TOFs calculated based on ratio of H_2/CO_2.

^{31}P NMR showed the decomposition of [Ru(κ^3-CNN)(dppb)Cl] in acidic environment (Figure 1). However, another major Ru species with two doublets at 47.63 (d, J = 28.5 Hz, 1P) and 43.40 ppm (d, J = 28.5 Hz, 1P) can be observed, which still dehydrogenates FA as shown in Table 1 (entry 1). Applying basic conditions resulted in two main complexes. On the one hand, [Ru(κ^3-CNN)(dppb)Cl] **6** with two doublets at 56.87 (d, J = 38.5 Hz, 1P) and 42.05 ppm (d, J = 38.5 Hz, 1P) is observed. Secondly, the [Ru(κ^3-CNN)(dppb)(OOCH)] **8** formate complex is formed showing a doublet at 59.59 (d, J = 38.4 Hz, 1P) and 42.09 ppm (d, J = 38.4 Hz, 1P) (Figure S14 and Figure S15) [28]. This suggests that the Ru–C bond is stable under basic conditions. It is worth mentioning that the main reason for the ruthenium–carbon bond (Ru–C) not to cleave is the tridentate coordination mode of the ligand (κ^3-CNN). Indeed, the Ru–C bond is much stronger thanks to the κ^2-aminopyridine moiety coordinated to the ruthenium center. On another hand, the -NH_2 moiety remains and is not deprotonated under basic condition ruling out a ruthenium amido complex, Ru=NH. Furthermore, the obtained [Ru-OOCH] complex is one of the major species involved in the catalytic cycle for the FA DH. Additional NMR experiments were carried out in toluene-d^8 and benzene-d^6 to identify the corresponding ruthenium hydrides such as [Ru(κ^3-CNN)(dppb)(H)], but we could not observe it (Figure S16). The recorded ^{1}H NMR also confirmed the presence of the complexes [Ru(CNN)(dppb)Cl] **6** and [Ru(κ^3-CNN)(dppb)(OOCH)] **8** in basic conditions. Again, applying acidic conditions led to decomposition of complex **6** and several signals were detected in the hydride region at –9.21, –10.67, –12.91 and –15.78 ppm. Those signals might be attributed to ruthenium hydride [Ru-H] or ruthenium hydrogen [Ru-H_2] complexes chelated by bisphosphine ligands as described in previous systems (Figure S17) [29]. Carrying H^{13}COONa labelling NMR experiments allowed observation of the formate signal in ^{13}C NMR. [Ru(κ^3-CNN)(dppb)(OO^{13}CH)] was observed at 170.75 ppm (Figure S18). The content of the NMR tube (DCM-d^2) was overlayered with diethyl ether (Et_2O) in a Schlenk flask and stored at - 20 °C. After several days, we got crystals for X-ray crystallography (Figure S13 and Figure S21) from the HCOOH and HCOOK reactions.

Despite the poor X-ray diffraction data and thus limited structure refinement of obtained complex **7** (Figure S13), we can state that the CNN ligand cleaves off. Apparently, a formate-dichloride bridged ruthenium dimer was formed with a dppb moiety coordinating each metal center. Similar complex: [Ru_2(μ-Cl)$_2$(μ-OOCMe)(PPh_3)$_4$][B(PPh_3)$_4$], has been reported [30]. Crystals resulting from the reaction under basic conditions are identified as complex **8** (Figure S13 and Scheme S3), described and characterized by Baratta and co-workers [28]. Abstraction of the chloride by a formate entity leads to [Ru(CNN)(dppb)(OOCH)], a key species in the catalytic cycle. To confirm this, the latter complex was tested in the FA DH, too (Figure 2).

To our delight, [Ru(κ^3-CNN)(dppb)(OOCH)] afforded slightly higher productivity compared to [Ru(κ^3-CNN)(dppb)Cl] with a TON of 9085 in 180 minutes (944 mL of H_2/CO_2 mixture, ratio vol.%H_2/(vol.%H_2+vol.%CO_2) = 0.71). Based on all these observations, we propose the following catalytic cycle for the Ru

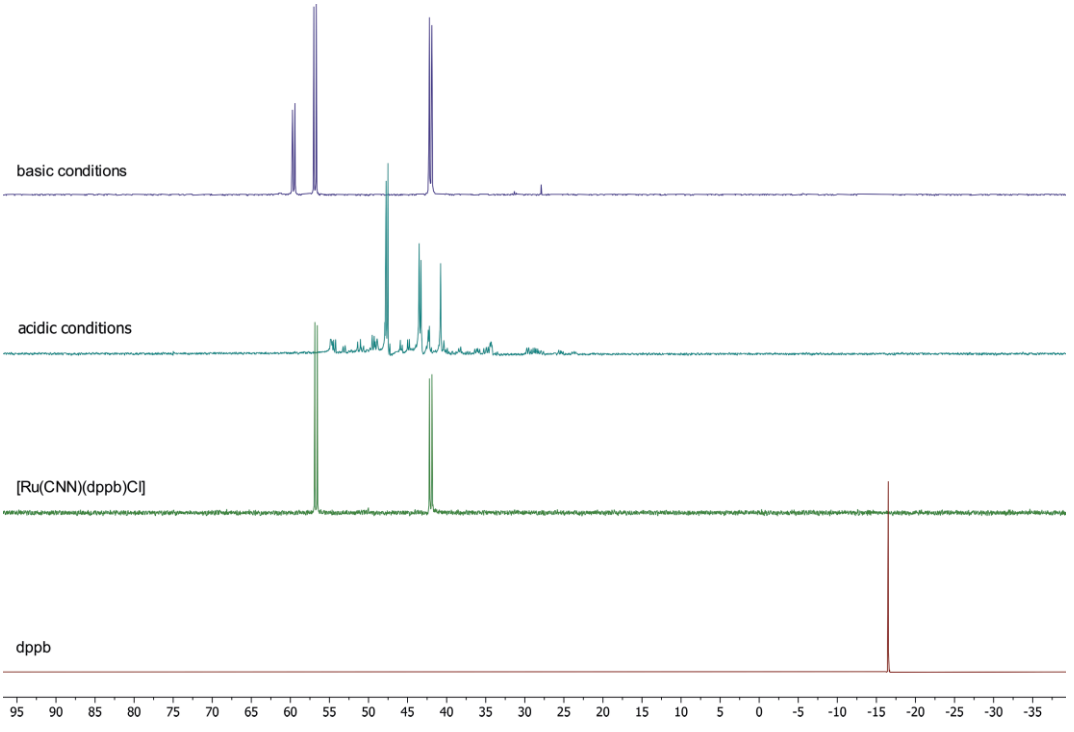

Figure 1. Stacked ^{31}P NMR experiments. Reaction conditions for acidic medium: HCOOH (0.08 mL), DCM-d^2 (1 mL), [Ru(CNN)(dppb)Cl] (0.04 mmol), T_{set} (40 °C), time (60 min). Reaction conditions for basic medium: HCOOK (166 mg), DCM-d^2 (1 mL), D_2O (1 mL), [Ru(CNN)(dppb)Cl] (0.04 mmol), T_{set}(40 °C), time (60 min). The content of the gas phase was analyzed by gas chromatography (GC). H_2, CO_2 and CO were observed in the gas phase.

Full Paper
doi.org/10.1002/ejic.202000068

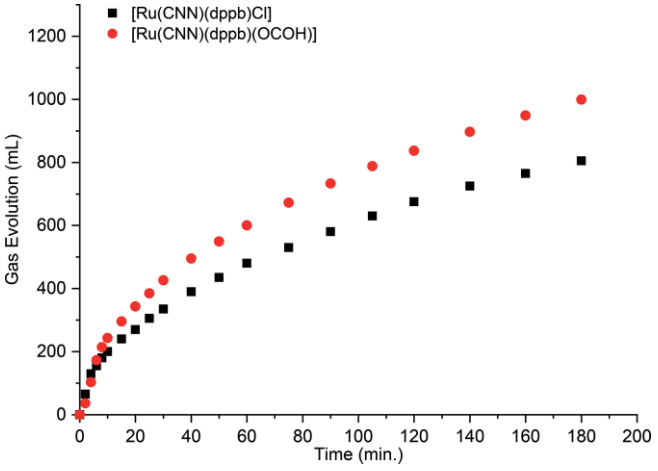

Figure 2. Tested [Ru(CNN)(dppb)(OOCH)] for the FA DH. Reaction conditions: HCOOH (37 mmol), KOH (40 mmol), Cat. (3 μmol), H_2O (9 mL), trigylme (4 mL), T_{set} (92 °C), time (180 min). Gas evolution monitored with manual burettes, corrected by blank volume (2.2 mL) and content of the gas phase analyzed by gas chromatography (GC). Ratio vol.%H_2/(vol.%H_2 +vol.%CO_2)of 0.71 for [Ru(CNN)(dppb)(OOCH)] and 0.67 for [Ru(CNN)(dppb)Cl] (Table S1). CO was not observed in the gas phase (detection limit 10 ppm) (Table S1). Experiments were performed twice with reproducibility differences between 2.1 and7.9%.

catalyzed DH of FA bearing a coordinated cyclometalated κ^3-CNN ligand (Scheme 4).

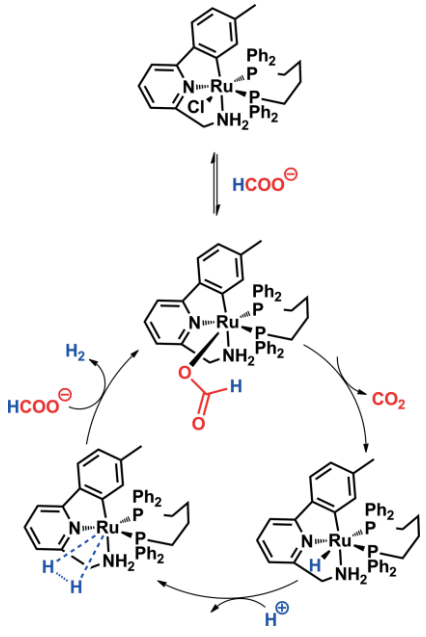

Scheme 4. Proposed mechanism for the FA dehydrogenation under basic conditions.

Addition of formate leads to the abstraction of the chloride resulting in the complex: [Ru(κ^3-CNN)(dppb)(OOCH)]. Such formate complexes are generally depicted as a key species in DH of FA [3, 31]. Next, β-hydride elimination leads to [Ru(κ^3-CNN)(dppb)H] and CO_2. For this reaction, the latter step has been previously demonstrated to be rate limiting [31]. Additionally, Baratta et al. described the β-hydride elimination leading to the hydride complex, in transfer hydrogenation reactions[31]. Finally, protonation of the hydride complex leads to Ru-H_2 species which regenerates [Ru(κ^3-CNN)(dppb)(OOCH)] liberating H_2, as described by Milstein et al [32]. and others[2].

Extended Catalyst Iterative Investigation

We were interested in investigating the impact and the importance of the cyclometalated ligand and more precisely the stability of the Ru–C bond. In this context, a selection of ruthenium complexes was synthesized or bought from suppliers (Scheme 5) and tested for the FA DH (Table 3).

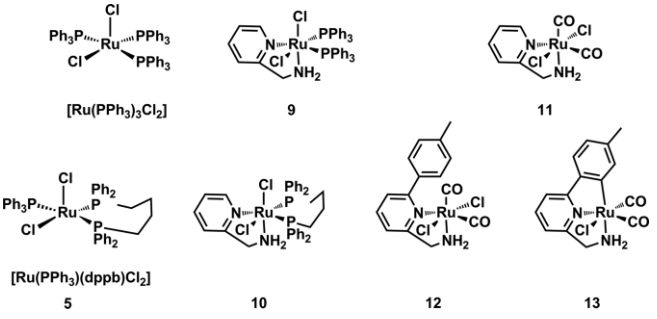

Scheme 5. Additional ruthenium complex synthesized.

Table 3. Catalyst variation for the DH of FA.[a]

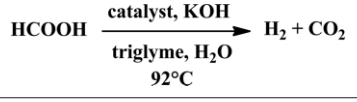

Entry	Catalyst	Volume [mL]	TON[b]	TOF[c]
1	6	817	7414	2471
2	[$Ru(PPh_3)_3Cl_2$]	99	831	277
3	5	140	819	318
4	9	172	1173	391
5	10	120	752	274
6	11	45	306	102
7	12	29	197	66
8	13	29	197	66

[a] Reaction conditions: HCOOH (37 mmol), triglyme (4 mL), water (9 mL), KOH (40 mmol), catalyst (3 μmol), T_{set} (92 °C), time (180 min). Gas evolution was monitored with manual burettes, corrected by blank volume (2.2 mL) and content of the gas phase analyzed by gas chromatography (GC). Ratio vol.-%H_2/(vol.-%H_2 +vol.-%CO_2) of 0.5 except entries 1, 2, 3 and 5 (0.67, 0.62, 0.43 and 0.46) (Table S1). CO was not observed in the gas phase (detection limit 10 ppm) except from entries 6, 7 and 8 (222, 93 and 25 ppm respectively) (Table S1). Experiments in entries 1, 5 and 8 were performed twice with reproducibility differences between 2.1 and 9.1 %. [b] TONs and TOFs calculated based on ratio of H_2/CO_2. [c] TOFs calculated after 3 hours.

In the absence of the CNN ligand, complexes [$Ru(PPh_3)_3Cl_2$] (entry 2) and [$Ru(PPh_3)$(dppb)Cl] (entry 3) showed a significantly lower productivity than their homologue [Ru(κ^3-CNN)(dppb)Cl] (entry 1). The productivity dropped drastically when [Ru(AMP)(dppb)Cl_2] (AMP = 4-(aminomethyl)pyridine) (entry 4) and [Ru(AMP)$(PPh_3)_2Cl_2$] (entry 5) were used instead of [Ru(CNN)(dppb)Cl] demonstrating the benefit of the cyclometalated κ^3-CNN bonding mode on the ruthenium.

In the context of environmentally benign catalytic processes, phosphine free catalytic systems are interesting. In part inspired by the fact that CO is essential in the reported

Full Paper
doi.org/10.1002/ejic.202000068

[Ru(^{iPr}P^{Me}N^{iPr}P)CO(H)Cl] complex for the FA DH(TOF = 2598, 99% conversion in 3 hours), we synthesized complexes **11–13** [25]. Unfortunately, [Ru(AMP)$(CO)_2Cl_2$] yielded a low TON of 306 (entry 6). The similar [Ru(κ^2-CNN)$(CO)_2Cl_2$] led to an even lower TON of 197, that can be explained by increased steric hindrance (entry 7). Finally, a TON of 197 was reached in 3 hours using [Ru(κ^3-CNN)$(CO)_2$Cl] (entry 8), which remains significantly lower than [Ru(κ^3-CNN)(dppb)Cl] (TON of 7414, entry 1). Interestingly, for carbonyl-based complexes **11**, **12** and **13**, high CO production was observed: 222, 93 and 25 ppm, respectively (entries 6, 7 and 8). This might be due to the CO ligand cleavage from the metal or the dehydration reaction being favored (HCOOH → CO + H_2O, aka decarbonylation of FA). On another hand, synthesis of [Ru(κ^3-CNN)(bpy)Cl] was attempted but ended up being unsuccessful. [Ru$(PPh_3)_2$(bpy)Cl_2] was obtained but coordination of the κ^3-CNN ligand did not occur.

Conclusions

The dehydrogenation of formic acid catalyzed by cyclometalated κ^3-CNN ruthenium complexes was investigated under acidic, neutral, and basic conditions. Catalyst **8**, [Ru(κ^3-CNN)(dppb)(OOCH)], showed a high turnover number of 9085 in 180 minutes under optimal conditions. Almost full conversion was achieved after 25 hours in aqueous/trigylme conditions using catalyst **6**, [Ru(κ^3-CNN)(dppb)Cl] (96%, TON = 11 910). NMR investigation and gas evolution experiment showed that the ligand is released under acidic conditions. In neutral and basic media, the κ^3-CNNremains coordinated and the complex **8**, [Ru(κ^3-CNN)(dppb)(OOCH)], is probably the key species in the catalytic cycle. Additional experiments revealed that increasing the temperature led to higher H_2 and CO_2 production along with higher CO content. Variations of catalytic loading and additive use were not beneficial to the reaction.

Experimental Section

Material and methods: Unless otherwise noted, all reagents were purchased from commercial sources and directly used without any further purification. Every reaction was carried out under an inert atmosphere using standard double Schlenk line technique. Formic acid (99–100 % purity) was purchased from BASF. In order to remove eventual impurities or stabilizers, triglyme and N,N-dimethyl-*N*-octylamine (DMOA) were previously distilled. Formic acid (FA), N,N-dimethyl-N -octylamine (DMOA), triglyme, triethylamine and water were all degassed wit argon (Ar) prior to use. Every organic solvent used in synthesis was collected from an SPS machine, stored under argon with drying agent (molecular sieves 4 Å) and degassed. All synthesized complexes were prepared under an argon atmosphere and stored under argon. Thin layer chromatography – TLC – was performed on aluminum backed hand-cut silica plates (5 cm × 10 cm, TLC Silicagel 60 F254, Merck Millipore) and visualized using ultraviolet light (wavelength: 254 nm). Column chromatography was done on using silica (0.035–0.070 mm, Silicagel 60, Fluka Chemika). The solvents were purchased from commercial sources used without any further purification. ^{1}H, ^{13}C and ^{31}P NMR spectroscopy were carried out on Bruker AV-300, AV-400 or f300 spectrometer. NMR spectrums were interpreted using MestReNova (version 8.0.1–10878). All NMR data, in the manuscript and in the ESI experimental, are expressed as chemical shift in parts per million (ppm) relative to the residual solvent used as an internal standard for the δ scale. The multiplicity of each signal is designed as follow; s (singlet), d (doublet), t (triplet), b (broad), m (multiplet). Infrared spectrometry was carried out with a Bruker-ALPHA FT-IR spectrometer with a spectral range of 7500 to 375 cm-1 (wavelength range: 1.3 to 27 mm). The solids were analyzed by ATR – Attenuated Total Reflectance – sampling method and the spectrums are exploited on OMNIC 7.3 or Origins 8.6. Gas chromatography was used to analyze the content of the gas phase with a CO quantification limit of 10 ppm. The samples were analyzed on Agilent Technologies 6890N GC system (HP Plot Q/FID – hydrocarbons, Carboxen/TCD – permanent gases, He carrier gas.). X-ray structure analyses were carried out on Bruker Kappa APEX II Duo diffractometer. Synthesis of (6-(*p*-tolyl)pyridin-2-yl)methanamine **4**, complexes [$RuCl_2(PPh_3)$(dppb)] **5**, [Ru(κ^3-CNN)(dppb)Cl] **6**, [Ru(κ^3-CNN)(dppb)(OOCH)] **8**, [*cis*-Ru(AMP)$(PPh_3)_2$Cl], [trans-Ru(AMP)$(PPh_3)_2$Cl] **9**, [Ru(AMP)(dppb)Cl] **10**, $[RuCl_2CO_2]_n$, [Ru(AMP)$(CO)_2$Cl] **11**, [Ru(κ^2-CNN)$(CO)_2$Cl] **12**, [Ru(κ^3-CNN)$(CO)_2$Cl] **13**, [Ru(bpy)$(PPh_3)_2$Cl] and the unsuccessful attempt of [Ru(κ^3-CNN)(bpy)Cl] were all done according to reported literature and their synthesis are reported in the supporting information provided along with analytical data.

Typical procedure for the formic acid dehydrogenation:

A double walled reactor was equipped with a double burette manual set-up. The set up was purged with argon several times then potassium hydroxide (KOH), water (H_2O), triglyme (MeO$[CH_2O]_3$Me) and formic acid (HCOOH) were successively added. The reaction mixture was heated to the desired temperature was left to equilibrate under argon for 60 minutes. The catalyst was added in a mini-Teflon cup and the gas evolution was monitored.

Supporting Information (see footnote on the first page of this article): General methods, equipment, procedures, calculation of TON and TOF, gas evolution plots, analytical data, ligand synthesis, crystallographic data for the intermediate [Ru(κ^3-CNN)(dppb)-(OOCH)].

Abbreviations

Formic Acid (FA), Dehydrogenation (DH), Gas Chromatography (GC), Turnover Number (TON), Turnover Number Frequency (TOF), Nuclear Magnetic Resonance (NMR), Transfer Hydrogenation (TH), Dimethyloctylamine (DMOA), AMP (4-(aminomethyl)pyridine), Dichloromethane (DCM).

Acknowledgments

We thank all members of the research group "catalysis for energy" (LIKAT), Maximilian Marx, Dr. Pavel Ryabchuk, and Dr. Elisabetta Alberico for scientific discussion and valuable suggestions. We thank PD Dr. W. Baumann and Dr. A. Spannenberg for their technical and analytical support (all from LIKAT).

Keywords: Renewable energy · Hydrogen storage · Formic acid dehydrogenation · Ruthenium · Homogeneous catalysis

[1] For recent reviews see e.g.: a) K. Sordakis, C. Tang, L. K. Vogt, H. Junge, P. J. Dyson, M. Beller, G. Laurenczy, *Chem. Rev.* **2018**, *118*, 372–433; b) K. Alig, M. Fritz, S. Schneider, *Chem. Rev.* **2019**, *119*, 2681–2751; c) W.-H. Wang, Y. Himeda, J. T. Muckerman, G. F. Manbeck, E. Fujita, *Chem. Rev.* **2015**, *115*, 12936–12973; d) P. G. Alsabeh, D. Mellman, H. Junge, M. Beller, *Top. Organomet. Chem.* **2014**, *48*, p. 45–80, Springer-Verlag Berlin Heidelberg **2014**; e) E. Alberico, L. K. Vogt, N. Rockstroh, H. Junge, In: Robert

J. Klein Gebbink, Marc-Etienne Moret (Eds.), *Non-Noble Metal Catalysis: Molecular Approaches and Reactions*, Wiley-VCH Verlag GmbH & Co. KGaA; Weinheim, Germany; **2019**, chapter 17, pp. 453–488.

[2] a) S.-F. Hsu, S. Rommel, P. Eversfield, K. Muller, E. Klemm, W. R. Thiel, B. Plietker, *Angew. Chem. Int. Ed.* **2014**, *53*, 7074–7078; *Angew. Chem.* **2014**, *126*, 7194; b) A. Boddien, C. Federsel, P. Sponholz, D. Mellmann, R. Jackstell, H. Junge, G. Laurenczy, M. Beller, *Energy Environ. Sci.* **2012**, *5*, 8907–8911; c) C. Guan, D.-D. Zhang, Y. Pan, M. Iguchi, M. J. Ajitha, J. Hu, H. Li, C. Yao, M.-H. Huang, S. Min, J. Zheng, Y. Himeda, H. Kawanami, K.-W. Huang, *Inorg. Chem.* **2017**, *56*, 438–445; d) S. Y. De Boer, T. J. Korstanje, S. R. La Rooij, R. Kox, J. N. H. Reek, J. V. Van Der Vlugt, *Organometallics* **2017**, *36*, 1541–1549.

[3] a) W.-H. Wang, M. Z. Ertem, S. Xu, N. Onishi, Y. Manaka, Y. Suna, H. Kambayashi, J. T. Muckerman, E. Fujita, Y. Himeda, *ACS Catal.* **2015**, *5*, 5496–5504; b) N. Onishi, R. Kanega, E. Fujita, Y. Himeda, *Adv. Synth. Catal.* **2018**, *360*, 1–9; c) P. Zhang, Y.-J. Guo, J. Chen, Y.-R. Zhao, J. Chang, H. Junge, M. Beller, Y. Li, *Nature Catal.* **2018**, *1*, 332–338; d) J. J. A. Celaje, Z. Lu, E. A. Kedzie, N. J. Terrile, J. N. Lo, T. J. Williams, *Nat. Commun.* **2018**, *7*, 1–6.

[4] a) A. Boddien, D. Mellmann, F. Gärtner, R. Jackstell, H. Junge, P. J. Dyson, G. Laurenczy, R. Ludwig, M. Beller, *Science* **2011**, *333*, 1733–1736; b) A. Boddien, B. Loges, F. Gärtner, C. Torborg, K. Fumino, H. Junge, R. Ludwig, M. Beller, *J. Am. Chem. Soc.* **2010**, *132*, 8924–8934; c) I. Mellone, N. Gorgas, F. Bertini, F. Peruzzini, K. Kirchner, L. Gonsalvi, *Organometallics* **2016**, *35*, 3344–3349; d) R. Langer, Y. Diskin-Posner, G. Leitus, L. J. W. Shimon, Y. Ben-David, D. Milstein, *Angew. Chem. Int. Ed.* **2011**, *50*, 9948–9952; *Angew. Chem.* **2011**, *123*, 10122; e) E. Bielinski, P. O. Lagaditis, Y. Zhang, B. Q. Mercado, C. Würtele, W. H. Bernskoetter, N. Hazari, S. Schneider, *J. Am. Chem. Soc.* **2014**, *136*, 10234–10237; f) A. Boddien, F. Gärtner, R. Jackstell, H. Junge, A. Spannenberg, W. Baumann, R. Ludwig, M. Beller, *Angew. Chem. Int. Ed.* **2010**, *49*, 8993–8996; *Angew. Chem.* **2010**, *122*, 9177.

[5] a) N. H. Anderson, J. Boncella, A. M. Tondreau, *Chem. Eur. J.* **2019**, *25*, 1–5; b) A. M. Tondreau, J. M. Boncella, *Organometallics* **2016**, *35*, 2049–2052; c) M. Andérez-Fernández, L. K. Vogt, S. Fisher, W. Zhou, H. Jiao, M. Garbe, S. Elangovan, K. Junge, H. Junge, R. Ludwig, M. Beller, Angew. Chem. Int. Ed. 2017, 56, 599–562; d) A. Léval, A. Agapova, C. Steinlechner, E. Alberico, H. Junge, M. Beller, Green. Chem. 2020, 22, 913–920.

[6] W. Zhou, W. Wie, A. Spannenberg, H. Jiao, K. Junge, H. Junge, M. Beller, *Chem. Eur. J.* **2019**, *25*, 8459–8464.

[7] a) T. Nakajima, Y. Kamiryo, M. Kishimoto, K. Imai, K. Nakamae, Y. Ura, T. Tanase, *J. Am. Chem. Soc.* **2019**, *141*, 8732–8736; b) N. Scotti, R. Psaro, N. Ravasio, F. Zaccheria, *RSC Adv.* **2014**, *4*, 61514–61517.

[8] a) M. C. Neary, G. Parkin, *Dalton Trans.* **2016**, *45*, 14645; b) S. Enthaler, A. Brück, A. Kammer, A. Junge, E. Irran, S. Gülak, *ChemCatChem* **2015**, *7*, 65–69.

[9] M. Vogt, A. Nerush, Y. Diskin-Posner, Y. Ben-David, D. Milstein, *Chem. Sci.* **2014**, *5*, 2043–2051.

[10] a) Z. Wang, S.-M. Lu, J. Wu, C. Li, J. Xiao, *Eur. J. Inorg. Chem.* **2016**, 490–496; b) Y. Himeda, S. Miyazawa, T. Hirose, *ChemSusChem* **2011**, *4*, 487–493.

[11] C. Chauvier, A. Tlili, C. Das Neves Gomes, P. Thuéryaand, T. Cantat, *Chem. Sci.* **2015**, *6*, 2938–2942.

[12] T. W. Myers, L. A. Berben, *Chem. Sci.* **2014**, *5*, 2771–2777.

[13] T. P. Rieckborn, E. Huber, E. Karakoc, M. H. Prosenc, *Eur. J. Inorg. Chem.* **2010**, *2010*, 4757–4761.

[14] B. Loges, A. Boddien, H. Junge, M. Beller, *Angew. Chem. Int. Ed.* **2008**, *47*, 3962–3965; *Angew. Chem.* **2008**, *120*, 4026.

[15] C. Fellay, P. J. Dyson, G. Laurenczy, *Angew. Chem. Int. Ed.* **2008**, *47*, 3966–3968; *Angew. Chem.* **2008**, *120*, 4030.

[16] a) Y. Gao, J. Kuncheria, G. P. A. Yap, R. J. Puddephatt, *Chem. Commun.* **1998**, 2365–2366; b) Y. Gao, J. K. Kuncheria, H. A. Jenkins, R. J. Puddephatt, G. P. A. Yap, *J. Chem. Soc., Dalton Trans.* **2000**, 3212–3217; c) A. Boddien, B. Loges, H. Junge, F. Gärtner, J. R. Noyes, M. Beller, *Adv. Synth. Catal.* **2009**, *351*, 2517–2520; d) P. Sponholz, D. Mellmann, H. Junge, M. Beller, *ChemSusChem* **2013**, *6*, 1172–1176.

[17] a) A. Boddien, B. Loges, H. Junge, M. Beller, *ChemSusChem* **2008**, *1*, 751–758; b) H. Junge, A. Boddien, F. Capitta, B. Loges, J. R. Noyes, S. Gladiali, M. Beller, *Tetrahedron Lett.* **2009**, *50*, 1603–1606

[18] E. Peris, R. H. Crabtree, *Chem. Soc. Rev.* **2018**, *47*, 1959–1968.

[19] J. Kothandaraman, M. Czaun, A. Goeppert, R. Haiges, J.-P. Jones, R. B. May, G. K. S. Prakash, G. A. Olah, *ChemSusChem* **2015**, *8*, 1442–1451.

[20] Y. Pan, C.-L. Pan, Y. Zhang, H. Li, X. Min, X. Guo, B. Zheng, H. Chen, A. Anders, Z. Lai, J. Zheng, K.-W. Huang, *Chem. Asian J.* **2016**, *11*, 1357–1360.

[21] G. A. Filonenko, R. Van Putten, E. N. Schulpen, E. J. M. Hensen, E. A. Pidko, *ChemCatChem* **2014**, *6*, 1526–1530.

[22] C. Prichat, M. Trincado, L. Tan, F. Casas, A. Kammer, H. Junge, M. Beller, H. Grützmacher, ChemSusChem 2018, 11, 1–5.

[23] I. Mellone, M. Peruzzini, L. Rosi, D. Mellmann, H. Junge, M. Beller, L. Gonsalvi, *Dalton Trans.* **2013**, *42*, 2495–2501.

[24] a) W. Baratta, G. Chelucci, S. Gladiali, K. Siega, M. Toniutti, M. Zanette, E. Zangrando, P. Rigo, *Angew. Chem. Int. Ed.* **2005**, *44*, 6214–6219; *Angew. Chem.* **2005**, *117*, 6370; b) W. Baratta, E. Herdtweck, K. Siega, M. Toniutti, *Organometallics* **2005**, *24*, 1660–1669.

[25] A. Agapova, E. Alberico, A. Kammer, H. Junge, M. Beller, *ChemCatChem* **2019**, *11*, 1910–1914.

[26] E. Ochiai, *J. Org. Chem.* **1953**, *18*, 534–551.

[27] a) W. Baratta, M. Ballico, S. Baldino, G. Chelucci, E. Herdtweck, K. Siega, S. Magnolia, P. Rigo, *Chem. Eur. J.* **2008**, *14*, 9148–9160; b) M. Solinas, B. Sechi, S. Baldino, W. Baratta, G. Chelucci, *ChemistrySelect* **2016**, *1*, 2492–2497.

[28] W. Baratta, M. Ballico, A. Del Zotto, E. Herdtweck, S. Magnolia, R. Peloso, K. Siega, M. Toniutti, E. Zangrando, P. Rigo, *Organometallics* **2009**, *28*, 4421–4430.

[29] K. Sordakis, M. Beller, G. Laurenczy, *ChemCatChem* **2014**, *6*, 96–99.

[30] A. M. Rheingold, A. Getty, *CSD Communication* **2015**, CCDC 1441040.

[31] M. Iglesias, L. A. Oro, *Eur. J. Inorg. Chem.* **2018**, *2018*, 2125–2138.

[32] T. Zell, B. Butschke, Y. Ben-David, D. Milstein, *Chem. Eur. J.* **2013**, *19*, 8068–8072.

Received: January 23, 2020